Available online at www.sciencedirect.com

SCIENCE DIRECT®

ELSEVIER

Journal of Nuclear Materials 329–333 (2004) 1142–1146

journal of nuclear materials

www.elsevier.com/locate/jnucmat

Mechanical characterization of austenitic stainless steel ion irradiated under external stress

I. Ioka [a,*], M. Futakawa [a], A. Naito [a], Y. Nanjyo [a], K. Kiuchi [a], T. Naoe [b]

[a] *Department of Nuclear Energy System, Japan Atomic Energy Research Institute, 2-4 Shirakata, Tokai-mura, Naka-gun, Ibaraki-ken 319-1195, Japan*

[b] *Ibaraki University, Hitachi-shi, Ibaraki-ken 316-8511, Japan*

Abstract

In a neutron irradiation field, irradiation creep takes place at temperatures far below the temperature that would cause significant thermal creep. It is expected that irradiation creep will cause the degradation of mechanical properties. The mechanical properties of type 304 stainless steel irradiated under external stress were examined using a nanoindentation technique combined with inverse analysis by a finite element method. The specimens were irradiated at a temperature of 300 °C under external stress using the triple ion beam facility. The degree of hardening for the irradiated specimen did not depend on the external stress. From the analytical results, there is little influence of applied stress on yield stress and nominal stress–strain curve of the irradiated specimen in this test condition.

1. Introduction

Irradiation creep has been studied extensively to provide data that can be used for component analysis of fusion, fast breeder and light water reactors. It is now generally recognized that the irradiation creep data were in agreement with an empirical equation [1]. Moreover, there have been many irradiation experiments done under applied stress to investigate stress effects on microstructural evolution. It is reported that the total nucleation rate of Frank loops was increased with increasing external stress [2]. However, there are few studies on the effect of external stress on mechanical properties of the material under irradiation.

The absence of a neutron source with fully fusion relevant neutron spectra requires that experimental studies must use surrogate irradiation facilities. A triple ion irradiation can be used for simulating the effect of irradiation on the mechanical properties of materials. The ion irradiation can simulate the irradiation environment by producing displacement damage in the material while simultaneously implanting H and He, which are controlled to achieve the equivalent dpa to the irradiation damage expected for fusion. However, the ion-irradiated area is limited to the very shallow surface layer (<2 μm depth) of the specimen so that the irradiation damage is distributed in a thin layer. Hence, a nanoindentation technique combined with inverse analysis using a finite element method (FEM) was applied to examine the influence of ion irradiation on the mechanical properties of the thin layer and derive the constitutive equation of the damaged layer [3]. The purpose of this study is to evaluate the mechanical properties of the irradiated material under external stress.

2. Experimental procedure

2.1. Material

The material tested is type 304 stainless steel in the solution-annealed condition. The chemical composition is given in Table 1. The configuration of the specimen

---

* Corresponding author. Tel.: +81-29 282 6385; fax: +81-29 282 6489.

E-mail address: ioka@popsvr.tokai.jaeri.go.jp (I. Ioka).

0022-3115/$ - see front matter © 2004 Elsevier B.V. All rights reserved.
doi:10.1016/j.jnucmat.2004.04.038

and the ion irradiation holder for applying the required stress are shown in Fig. 1. The thickness of specimen is about 0.2 mm. It has three different cross sections (1.5, 1.75, 2.0 mm in width) in order to irradiate at different stress at the same time. The surface of specimen was polished with #2400 paper and then was electrochemically polished. The spring was used in order to apply the required stress in the specimen during irradiation. The strain gauge was attached at L division (2.0 mm in width) of the specimen to measure the tensile strain before ion irradiation. The spring was adjusted so that the tensile strain at L division may become about 0.2%. The applied stress, about 200 MPa, at L division was estimated from the stress–strain curve of type 304 SS. In this time, the applied stresses of M division (1.75 mm in width) and S division (1.5 mm in width) were about 228 and 266 MPa, which were calculated from each cross section. The strain of S and M divisions were estimated from strain–stress curve about 1% and 0.5%, respectively. The strain gauge was removed before irradiation.

The electrochemically polished specimens were irradiated in triple (12 MeV Ni^{3+}, 1.1 MeV He^{+} and 380 keV H^{+}) ion beam mode at a temperature of 300 °C using the triple ion beam facility (TIARA) at JAERI. The temperature of the specimen was measured by an infrared thermometer (THERMAL VISION, Nikon Co.). The temperature of the spring was less than 50 °C during irradiation at 300 °C. It is believed that the stress applied to the specimen is maintained during irradiation. The displacement damage in the specimen was mainly attributed to Ni^{3+} ion irradiation. The peak dose was about 10 dpa around 2 μm. The He^{+} and H^{+} ions were implanted in depth ranges from 1.0 to 1.5 μm using an aluminum foil energy degrader. The concentration of He^{+} and H^{+} ions in the implanted range were 11 appmHe and 91 appmH, which correspond to LWR condition. The dose was about 5 dpa in the implanted range of He^{+} and H^{+} ions.

2.2. Nanoindentation test

The nanoindentation technique may be applied to evaluate mechanical properties of the very shallow irradiated surface layer. The nanoindentation test was carried out on the surfaces of the irradiated and unirradiated specimens at room temperature. Two types of indenters were used for the nanoindentation test. One is the Berkovich indenter for measuring the hardness, the other is a conical indenter that has a hemispherical apex with radius of 1.2 μm for deriving the constitutive

Table 1
Chemical composition of the material tested in wt%

Materials	Fe	C	Si	Mn	P	S	Cr	Ni	Co
Type 304SS	Bal.	0.063	0.49	1.45	0.016	0.012	18.72	10.27	0.003

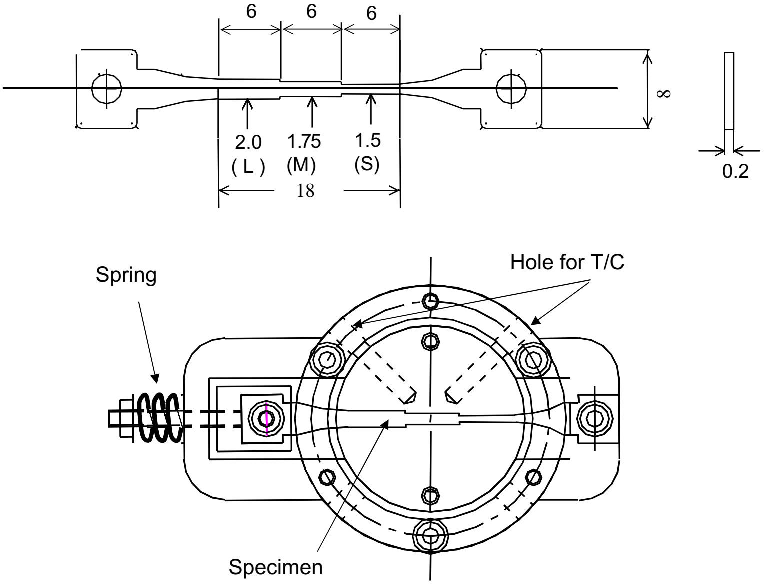

Fig. 1. Dimensions of the specimen designed for ion irradiation under external stress and configuration of the ion irradiation holder.

equation. A DUH-200 (Shimadzu Co.) testing machine was used for the nanoindentation test. The load was applied with a loading speed of 2.6×10^{-3} N/s, held 1 second and then removed. During loading and unloading, the load was continuously monitored along with the displacement with a resolution of 19.6 mN and 0.01 μm, respectively. The data obtained with the Berkovich indenter was converted into a relationship between load/depth and depth (*L*/*D*–*D* curve), and the hardness was evaluated from the slope of these curves.

2.3. FEM analysis

The interaction between the irradiated thin layer and substrate (unirradiated region) complicates the deformation under the indenter and makes it difficult to characterize the irradiated thin layer. An inverse analysis was carried out using an explicit FEM code, LS-DYNA [4], which enables us to roughly analyze a large deformation that accompanies contacting behavior. In the analysis, the indenter and specimen were treated as axisymmetric two-dimensional bodies to improve the efficiency of the calculation. The indenter was modeled as a perfectly rigid. The fineness of the mesh size is determined by the required accuracy. The minimum element size of 0.05 μm is near the apex contacting zone.

The constitutive equation of the material employed in the model was assumed to be a simple power-law which is generally believed to be applicable to normal metallic materials as follows:

$$\sigma = E\varepsilon, \quad \sigma \leqslant \sigma_y, \tag{1}$$

$$\sigma = A(\varepsilon_0 + \varepsilon)^n, \tag{2}$$

$$\varepsilon_0 = (\sigma_y/A)^{1/n} - (\sigma_y/E), \quad \sigma > \sigma_y, \tag{3}$$

where σ is true stress, ε true strain, E Young's modulus, σ_y yield stress, A work hardening coefficient and n work hardening exponent. Therefore, we have to identify the following material constants; σ_y, A and n through the inverse analysis on the *L*–*D* curve.

The flow chart of the inverse analysis is illustrated in Fig. 2. Here, **C** and **E** are determinants of material constants and estimated errors of material constants. **Z** and **Y** are determinants of experimental and calculated values on *L* and d*L*/d*D*. **R** is determinant of error in measuring systems. $S_{\max}$ is the maximum number of steps in the divided *L*–*D* curve. **H** is $\partial\mathbf{Y}/\partial\mathbf{C}$. The procedure of the inverse analysis is as follows:

(1) $\mathbf{C}_0, \mathbf{E}_0, \mathbf{R}$ and $S_{\max}$ are input as initial values.
(2) $\mathbf{Z}_s$ of *L* and d*L*/d*D* are input at step S.
(3) $\mathbf{Y}_s$ of *L* and d*L*/d*D* are calculated at step S by FEM code.

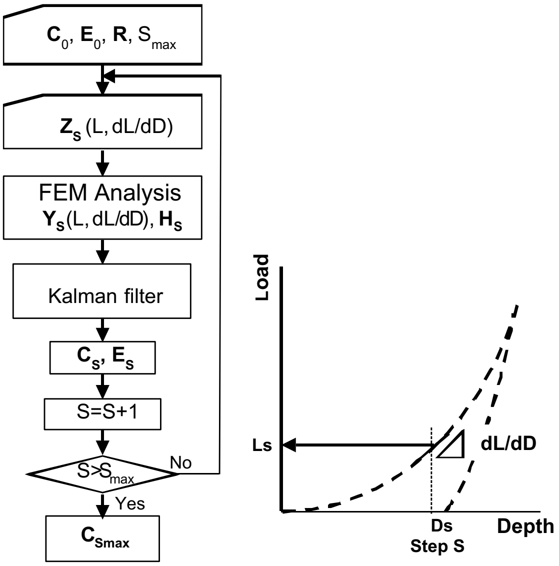

Fig. 2. Flow chart for identification of material constants.

(4) The estimated values of **C** and **E** are given by the following equation of the Kalman filter [5] using each value, $\mathbf{C}_s, \mathbf{E}_s, \mathbf{Y}_s, \mathbf{H}_s$ and **R** at step S,

$$\mathbf{C}_S = \mathbf{C}_{S-1} + \mathbf{E}_S\mathbf{H}_S\mathbf{R}^{-1}(\mathbf{Z}_S - \mathbf{Y}_S), \tag{4}$$

$$\mathbf{E}_S = \left(\mathbf{E}_{S-1}^{-1} + \mathbf{H}_S^T\mathbf{R}^{-1}\mathbf{H}_S\right)^{-1}. \tag{5}$$

(5) Go back to (2) and repeat the process up to $S_{\max}$. Finally we can obtain the optimal values $\mathbf{C}_{S_{\max}}$ estimated at final step $S_{\max}$.

3. Results and discussion

The *L*/*D*–*D* curves of the stress-free specimen before and after irradiation are shown in Fig. 3. The slope (straight solid and dotted lines in Fig. 3) of the *L*/*D*–*D* curve is in direct proportion to the hardness of the material. In the stress-free irradiated specimen, the slope up to 0.4 μm depth is higher than that at depth greater than 0.4 μm. The slope at depth greater than 0.4 μm is almost same as that of unirradiated one. It means that the irradiated layer (about 2 μm) affects the *L*/*D*–*D* response of the irradiated specimen up to 0.4 μm depth. This tendency was observed in another study using the same technique [6]. Fig. 4 shows the slope at depth greater than 0.4 μm in the S, M and L divisions of the stressed and the stress-free irradiated specimens. The slope in all divisions of the stressed–irradiated specimen was higher than that of the stress-free irradiated one. The slope in all divisions of the stressed–irradiated specimen was almost the same. It indicates the stressed–

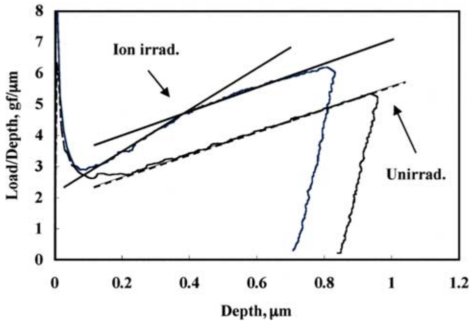

Fig. 3. *L*/*D*–*D* curves of stress-free specimens before and after irradiation.

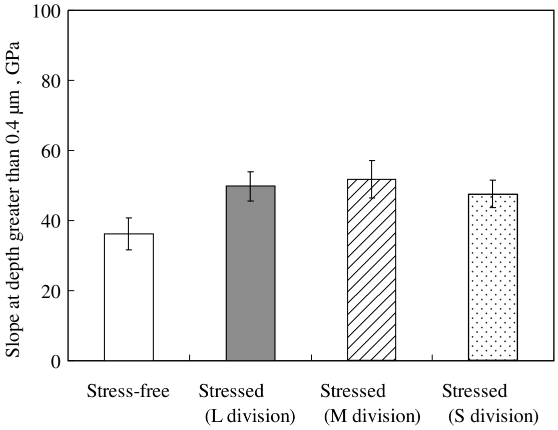

Fig. 4. Slope at depth greater than 0.4 μm in the S, M and L divisions of the stressed and the stress-free irradiated specimens.

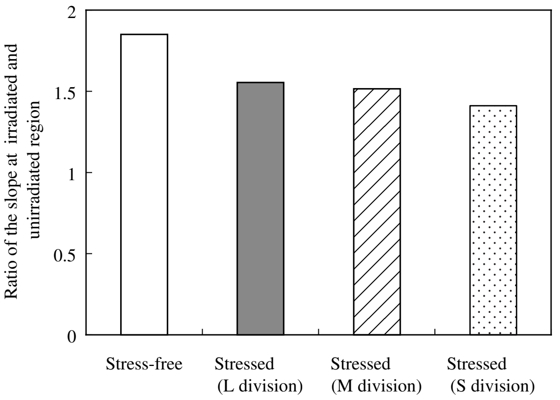

Fig. 5. Ratio of the slope in irradiated region (below 0.4 μm depth) to that of the unirradiated region (above 0.4 μm depth) in the S, M and L divisions.

irradiated specimen was plastically deformed during stressing. The result was in fair agreement with the result of tensile test that the yield stress was about 150 MPa. However, it is expected that the cold-worked level of S division was about 1% at most from the stress–strain curve.

From the slope of two lines below and above 0.4 μm depth, the change in hardness of the specimen by irradiation under external stress was calculated. Fig. 5 shows the ratio of the slope in the irradiated region (up to 0.4 μm depth) to that of the unirradiated region (greater than 0.4 μm depth) in the S, M and L divisions. The result for a stress-free specimen is added to Fig. 5. The irradiated layer of all specimens is hardened by irradiation. The ratio of the stress-free specimen was higher than those of the stressed specimen. It is well known that the increase in hardening of solution-annealed material is higher than that of cold-worked material in the same irradiated condition [7]. The degree of hardening did not depend on the external stress level in this test condition. The value of the applied stress in the S, M and L divisions was nearly the same. It is considered that little difference in hardening is attributed to the applied stress levels. So, the constitutive equation of irradiated layer was derived for division M since the hardness and *L*/*D*–*D* curves were almost the same in each division.

Fig. 6 shows the *L*–*D* curves measured using the conical indenter, and the calculated results using the material constants given in Eqs. (1)–(3) calculated by the inverse analysis method on the *L*–*D* curve. The calculated *L*–*D* curves agree well with the experimental ones as shown in Fig. 6. The material constants estimated from the inverse analyses on the *L*–*D* curves of the stressed and stress-free irradiated specimens are summarized in Table 2. The results of analysis for an unirradiated specimen are also shown in Table 2. It seems that the difference in the yield stress of the stressed and

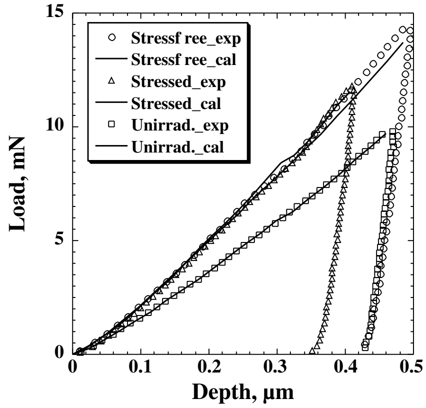

Fig. 6. *L*–*D* curves measured using the conical indenter and calculated results using the inverse analysis.

Table 2
Material constants estimated from the inverse analyses of irradiated layer with or without external stress

	Irradiated		Unirradiated
	Stress-free	Stressed (M division)	Stress-free
σ_y (MPa)	540	620	190
A (MPa)	1410	1350	1410
n	0.21	0.20	0.41

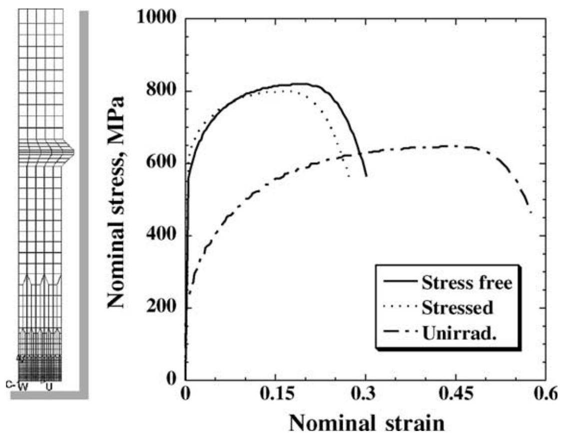

Fig. 7. Calculated nominal stress–strain curves of the stressed and stress-free irradiated specimens.

stress-free irradiated specimen is not remarkable considering the difference in the calculated and experimental yield stresses of the unirradiated specimen. The values of A and n were the same for both specimens. The value of n corresponds to uniform deformation of the material. So, it seems that the ductility loss of the irradiated specimens with or without applied stress is the same.

The constitutive equations identified for the irradiated layer with or without applied stress were used for the FEM analysis to obtain the stress–strain relationship. A two-dimensional axisymmetric model as shown in Fig. 7 was used for the analysis. The model has a high mesh density around the center of the specimen. The deformation of the specimen was calculated by LS-DYNA [4]. Fig. 7 shows the calculated nominal stress–strain curves of the irradiated specimen with or without applied stress. The analytical results indicated irradiation hardening and ductility loss from the very shallow irradiated layer. It is considered that there is little influence of applied stress on yield stress and nominal stress–strain curve of the irradiated specimen in this test condition.

4. Conclusion

The mechanical properties of type 304 austenitic stainless steel irradiated under external stress were examined using a nanoindentation technique combined with inverse analysis using a finite element method. The results of this study are summarized as follows:

(1) The degree of hardening did not depend on the external stress level in this test condition.
(2) From the analytical results, there is little influence of applied stress on yield stress and nominal stress–strain curve of the irradiated specimen in this test condition.

Acknowledgements

The authors wish to thank Mrs S. Suzuki and K. Tachibana for the preparation of specimens and the experiment.

References

[1] F.A. Garner, M.B. Toloczko, J. Nucl. Mater. 251 (1997) 252.
[2] H. Tanigawa, Y. Katoh, A. Kohyama, Nucl. Instrum. and Meth. B 102 (1995) 151.
[3] I. Ioka, M. Futakawa, Y. Nabjyo, T. Suzuki, K. Kiuchi, JAERI Rev. 35 (2002) 149.
[4] LS-DYNA User's Manual, Livermore Software Technology Corporation, 1995.
[5] S. Aoki, S. Kamaya, F. Terui, Trans. Jpn. Soc. Mech. Eng. A 64 (618) (1998) 445.
[6] Y. Katoh et al., J. Jpn. Inst. Met. 61 (1997) 191.
[7] M.L. Grossbeck, K. Ehrlich, C. Wassilew, J. Nucl. Mater. 174 (1990) 264.